# Formation of Hydroxyl Radicals from the Reaction of Water and Oxygen over Basic Metal Oxides

**Kevin B. Hewett, Louis C. Anderson, Michael P. Rosynek, and Jack H. Lunsford***

*Contribution from the Department of Chemistry, Texas A&M University, College Station, Texas 77843*

*Received February 21, 1996*[⊗]

**Abstract:** The reaction of water and oxygen to form hydroxyl radicals over the metal oxide catalysts $La_2O_3$, $Nd_2O_3$, $Sm_2O_3$, $Yb_2O_3$, $CeO_2$, and MgO was studied at pressures up to several Torr. After reaction over 27 mg of $La_2O_3$ at 900 °C, the measured concentration of hydroxyl radicals in the gas phase, detected by laser induced fluorescence spectroscopy, was equivalent to the expected equilibrium concentration. The reaction becomes kinetically controlled at catalyst loadings below 5 mg. Oxygen incorporation at the surface sites may be the rate limiting step in the catalytic cycle. The activities of the catalysts decrease from $La_2O_3$, the most active, to $CeO_2$, which is inactive under these reaction conditions. This order is the same as that found for methyl radical formation over these oxides, suggesting that the active site on the catalyst surface is the same for both hydroxyl radical formation and methyl radical formation.

## Introduction

One of the most common radical species observed in hydrocarbon combustion reactions is the hydroxyl radical ($OH^{\bullet}$). An important class of reactions is that which occurs during catalytic combustion where the hydroxyl radical serves as a radical chain carrier.[1−3] By increasing the steady-state concentration of hydroxyl radicals due to the presence of a catalyst, it is possible to lower the combustion temperature while still effecting complete hydrocarbon oxidation.[1−6] Moreover, formation of nitrogen oxides is greatly diminished at lower combustion temperatures. As a result, a variety of different catalysts have been studied for activity in producing hydroxyl radicals. These include metal surfaces,[7−12] supported metals,[13,14] and more recently the lanthanide oxides.[15]

The strongly basic lanthanide oxides generate methyl radicals during the reaction of methane with oxygen, and these catalysts have been shown to be both active and selective methane oxidative coupling catalysts.[16−18] The less basic lanthanide oxides, particularly those having multiple cationic oxidation states, were found to be complete combustion catalysts which produced few methyl radicals. It was also observed that over the most strongly basic lanthanide oxide, $La_2O_3$, hydroxyl radicals were produced during the reaction of methane and oxygen at pressures below 100 mTorr.[15] The radicals emanated into the gas phase where they were detected by laser induced fluorescence (LIF) spectroscopy. It was further demonstrated that the hydroxyl radicals were formed by the reaction of water, a product of the $CH_4$ oxidation reaction, and oxygen on the surface of the metal oxide. That is, methane was not required as a reagent. The surface-generated gas-phase hydroxyl radicals, produced from the reaction of water and oxygen, were observed to be in thermal and chemical equilibrium. Neodymium oxide, the only other strongly basic lanthanide oxide previously studied, also produced $OH^{\bullet}$ radicals, while the weakly basic lanthanide oxides such as $Yb_2O_3$ and $CeO_2$ were inactive for hydroxyl radical production. In the previous study, the pressure was limited to less than 100 mTorr so as to minimize secondary gas-phase reactions and to ensure that the rotational temperature of the radicals was the same as that of the surface.

In the present study, the reaction of water and oxygen over several lanthanide oxide catalysts was extended up to pressures of several Torr, which is a range more consistent with conventional kinetic studies. The pressure of the reactant gases, as well as the mass of catalyst used, was chosen such that the production of hydroxyl radicals was kinetically controlled. Thus, the activities of the catalysts could be compared and kinetic data could be obtained. The latter were used to gain insight into the mechanism of the surface-mediated reaction between water and oxygen.

## Experimental Section

The reactant gases consisted of three streams which were combined: oxygen, water-saturated helium, and a second pure helium

[⊗] Abstract published in *Advance ACS Abstracts,* July 1, 1996.

(1) Pfefferle, L. D.; Griffin, T. A.; Winter, M.; Crosley, D. R.; Dyer, M. J. *Combust. Flame* **1989**, *76*, 325−338.
(2) Vlachos, D. G.; Schmidt, L. D.; Aris, R. *AIChE J.* **1994**, *40*, 1005−1017.
(3) Vlachos, D. G.; Schmidt, L. D.; Aris, R. *AIChE J.* **1994**, *40*, 1018−1025.
(4) Trimm, D. L. *Appl. Catal.* **1983**, *7*, 249−282.
(5) Neyestanaki, A. K.; Lindfors, L.-E. *Combust. Sci. Technol.* **1994**, *97*, 121−136.
(6) Blazowski, W. S.; Walsh, D. E. *Combust. Sci. Technol.* **1975**, *10*, 233−244.
(7) Tevault, D. E.; Talley, L. D.; Lin, M. C. *J. Chem. Phys.* **1980**, *72*, 3314−3319.
(8) Talley, L. D.; Sanders, W. A.; Bogan, D. J.; Lin, M. C. *Chem. Phys. Lett.* **1981**, *78*, 500−503.
(9) Fujimoto, G. T.; Selwyn, G. S.; Kelser, J. T.; Lin, M. C. *J. Phys. Chem.* **1983**, *87*, 1906−1910.
(10) Ljungström, S.; Hall, J.; Kasemo, B.; Rosén, A.; Wahnström, T. *J. Catal.* **1987**, *107*, 548−556.
(11) Anderson, L. C.; Mooney, C. E.; Lunsford, J. H. *Chem. Phys. Lett.* **1992**, *196*, 445−448.
(12) Mooney, C. E.; Anderson, L. C.; Lunsford, J. H. *J. Phys. Chem.* **1993**, *97*, 2505−2506.
(13) Morrow, B. A.; Ramamurthy, P. *Can. J. Chem.* **1971**, *49*, 3409−3410.
(14) Morrow, B. A.; Ramamurthy, P. *J. Phys. Chem.* **1973**, *77*, 3052−3058.
(15) Anderson, L. C.; Xu, M.; Mooney, C. E.; Rosynek, M. P.; Lunsford, J. H. *J. Am. Chem. Soc.* **1993**, *115*, 6322−6326.
(16) Lin, C.-H.; Campbell, K. D.; Wang, J.-X.; Lunsford, J. H. *J. Phys. Chem.* **1986**, *90*, 534−537.
(17) Campbell, K. D.; Zhang, H.; Lunsford, J. H. *J. Phys. Chem.* **1988**, *92*, 750−753.
(18) Maitra, A. M. *Appl. Catal. A: General* **1993**, *104*, 11−59.

S0002-7863(96)00566-5 CCC: $12.00 

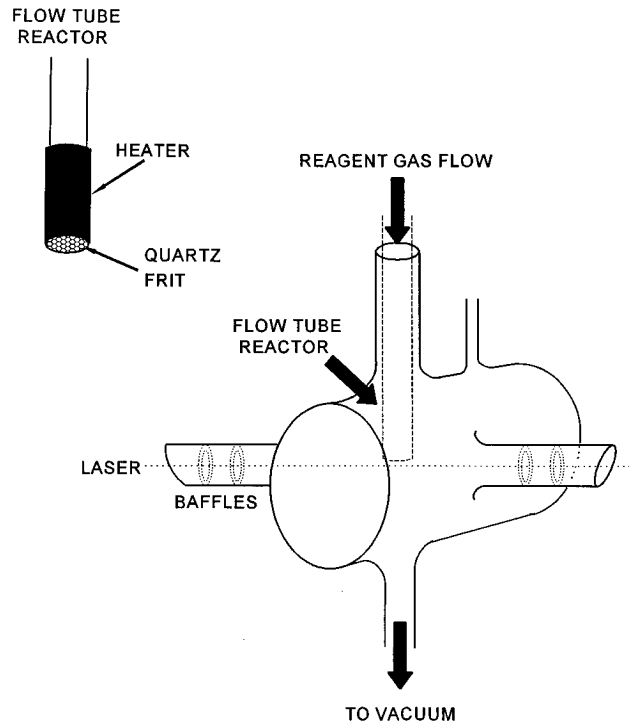


**Figure 1.** A schematic of the reaction cell showing the location of the laser beam and the catalyst.

stream. The partial pressure of water in the helium stream was controlled by adjusting the temperature of a liquid water saturator through which the helium was passed. The flow rates of all three gas streams were maintained by mass flow controllers.

The combined gas stream entered a reaction cell by passing through the flow tube reactor, as shown in Figure 1. The flow tube reactor consisted of a 10 mm i.d. fused-quartz tube which had a quartz frit attached to the end. A platinum resistance heating wire was wrapped around the lower ~5 cm of the tube and was covered by a high-temperature ceramic. The heated zone of the reactor was filled with quartz chips to preheat the reaction gases before they pass through the frit. The temperature was measured by a thermocouple on the inside of the reactor, touching the top of the frit and approximately 2.5 mm from the reactor wall. The catalyst to be studied was placed on the downstream surface of the frit.

Two methods of preparing the catalysts were used. The first method involved mixing the metal oxide with water to form a slurry. The slurry was then painted onto the quartz frit and allowed to dry. The catalyst was pretreated by heating to *ca.* 950 °C in vacuum for at least 6 h. This converted any metal hydroxide and carbonate to the metal oxide. The amount of catalyst was determined by weighing the frit before and after catalyst deposition.

In the second method, metal nitrates, which were dissolved in distilled water to form 0.4 M solutions, were used to prepare the catalysts. A known volume of the solution was placed, *via* a syringe, onto the frit and allowed to dry. The nitrate was converted into the oxide by heating to *ca.* 950 °C in 0.5 Torr of flowing $O_2$ for 9−12 h. The amount of catalyst present was determined by knowing the solution concentration and the volume placed onto the frit. Both methods of catalyst preparation resulted in metal oxides which quickly resulted in a steady state production of hydroxyl radicals.

The hydroxyl radicals formed on the catalyst surface were detected approximately 5 mm below the surface of the frit. The $A^2\Sigma^+(v=0) \leftarrow X^2\Pi(v=0)$ transition of the hydroxyl radicals, which occurs at *ca.* 308 nm, was excited by the frequency doubled output of a tunable dye laser (bandwidth ~0.3 $cm^{-1}$, pulse width 5 ns, energy ~0.2 mJ/pulse). The dye laser was pumped by the second harmonic of a Q-switched Nd:YAG laser operating at 10 Hz. The fluorescence was collected at 90° from the laser beam using two focusing lenses and detected using a photomultiplier tube (PMT). To ensure that only UV radiation was detected, an interference band-pass filter with a peak at 304.7 nm and a bandwidth of 29.4 nm was placed before the entrance slit of the PMT.

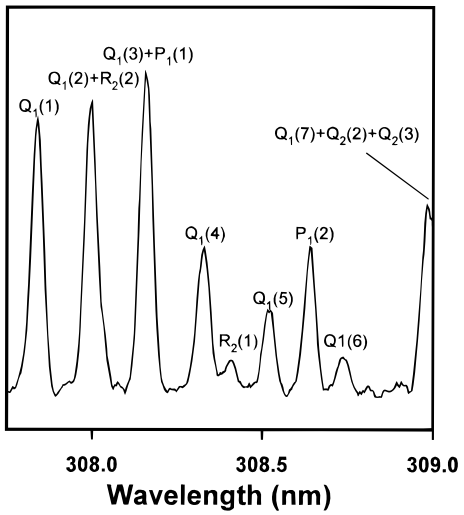


**Figure 2.** LIF spectrum of surface-generated gas-phase OH• radicals produced over $La_2O_3$ at 900 °C. The reagent gas pressures were 135.4 mTorr of $O_2$ and 39.6 mTorr of $H_2O$.

The output from the PMT was sent to a gated photon counter which was triggered by the Q-switch of the Nd:YAG laser.

For measuring the hydroxyl radical concentrations, two rotational lines, corresponding to the $Q_1(4)$ and $Q_1(5)$ transitions, were used. These were chosen since the amplitudes of these two lines relative to the total amplitude remained relatively constant over the temperature range of interest. The $Q_1(4)$ transition remained constant within 4.5% over the temperature range 800−1000 °C. In this same temperature range, the $Q_1(5)$ transition remained constant to within 2.5%. However, the signal-to-noise ratio of the $Q_1(4)$ peak was approximately twice that of the $Q_1(5)$ peak. Thus, at the large catalyst loadings on the strongly basic oxide catalysts, the $Q_1(5)$ transition was monitored to minimize errors due to temperature changes. On the weakly basic oxides and at low catalyst loadings on the strongly basic oxides, the smaller signal levels made the higher S/N ratio more important, and the $Q_1(4)$ transition was used.

## Results and Discussion

**Determination of OH• Concentration.** A portion of a typical hydroxyl radical spectrum is shown in Figure 2. The intensity of the selected rotational line, the intensity of Rayleigh scattering, and the rate constants for electronic quenching with reactant gases were used to determine the concentration of OH• radicals. As developed by Schofield and Steinberg,[19] the intensity of fluorescence can be represented as

$$I_f = n_{OH,i} \cdot \sigma_{OH,ij} \cdot V I_L \theta \cdot \frac{A_{ij}}{A_{ij} + \sum A_{im} + k_d + \sum k_q[M_q]} \quad (1)$$

where $n_{OH,i}$ is the number of hydroxyl radicals in the $i$th rotational state, $\sigma_{OH,ij}$ is the cross section for absorbing a photon and exciting the radical from the $i$th to the $j$th state, $V$ is the collection volume, $I_L$ is the laser intensity, $\theta$ is the collection efficiency, $A_{ij}$ is the Einstein $A$ coefficient for emission between the $i$ and $j$ states, $\Sigma A_{im}$ is the sum of the Einstein $A$ coefficients for undetected fluorescence (detector limitations), $k_d$ is the rate constant for predissociation, and $\Sigma k_q[M_q]$ is the sum of quenching rate constants times the concentration of the quenching agents.

The values for the collection volume, laser intensity, and collection efficiency are dependent upon the experimental apparatus. By utilizing the intensity of Rayleigh scattering from air at 25 °C and atmospheric pressure, these parameters could be eliminated from the calculation. Rayleigh scattering is

(19) Schofield, K.; Steinberg, M. *Opt. Eng.* **1981**, *20*, 501−510.

represented as:

$$I_{\mathrm{Ray}} = n_{\mathrm{Ray}} \cdot \sigma_{\mathrm{Ray}} \cdot V I_{\mathrm{L}} \theta \quad (2)$$

where $n_{\mathrm{Ray}}$ is the number of scattering particles and $\sigma_{\mathrm{Ray}}$ is the cross section for Rayleigh scattering. Combining eqs 1 and 2 and rearranging to give the number of hydroxyl radicals in the $i$th state:

$$n_{\mathrm{OH},i} = \frac{\sigma_{\mathrm{Ray}} n_{\mathrm{Ray}}}{\sigma_{\mathrm{OH},ij}} \cdot \frac{I_{\mathrm{f}}}{I_{\mathrm{Ray}}} \cdot \frac{A_{ij} + \sum A_{im} + k_{\mathrm{d}} + \sum k_{\mathrm{q}}[\mathrm{M_q}]}{A_{ij}} \quad (3)$$

Since the hydroxyl radical does not predissociate ($k_{\mathrm{d}} = 0$) and the detector bandwidth is large enough to detect all fluorescence ($\Sigma A_{im}=0$), eq 3 reduces further to:

$$n_{\mathrm{OH},i} = \frac{\sigma_{\mathrm{Ray}} n_{\mathrm{Ray}}}{\sigma_{\mathrm{OH},ij}} \cdot \frac{I_{\mathrm{f}}}{I_{\mathrm{Ray}}} \cdot \frac{A_{ij} + \sum k_{\mathrm{q}}[\mathrm{M_q}]}{A_{ij}} \quad (4)$$

Using the Boltzmann distribution and the results of eq 4, the total number of hydroxyl radicals located in the collection volume can be calculated. It was determined that the concentration of hydroxyl radicals decreased with increasing distance from the catalyst surface. This results from the fact that the radicals move away from the surface in a plume of increasing diameter. Between 3.5 and 19.4 mm the decrease in concentration followed a $1/r$ form. The hydroxyl radical concentration at the catalyst surface was determined by extrapolation to zero distance.

The hydroxyl radical absorption cross sections were obtained from McGee and McIlrath.[20] The Einstein $A$ coefficients used were those reported in the literature.[21−23] The values of the quenching rate constants were required in order to determine the value of the $\Sigma k_{\mathrm{q}}[\mathrm{M_q}]$ term in eq 4. Several studies have been performed to investigate the quenching rate constants for collisions between electronically excited hydroxyl radicals and various gases.[24−28] Some of these results are shown in Table 1. The rate constants used in this work to determine the OH• concentration were (in cm$^3$ molecules$^{-1}$ s$^{-1}$) $1.51 \times 10^{-10}$ for $O_2$, $5.42 \times 10^{-10}$ for $H_2O$, and $5.6 \times 10^{-14}$ for He. These are averages of the values in Table 1 and are assumed to be temperature independent over the temperature range studied. The values for $n_{\mathrm{Ray}}$ and the cross section $\sigma_{\mathrm{Ray}}$ were taken from ref 29.

**Production of OH• at Chemical Equilibrium.** Using a constant oxygen-to-water ratio of 3.7:1.0, the concentration of hydroxyl radicals produced over 27 mg of $La_2O_3$ was determined as a function of total pressure. The results of such an experiment are shown in Figure 3, from which it is evident that the OH• radical concentration, corrected for collisional quenching, was the same as the calculated equilibrium concentration within experimental error. The effect of collisional quenching was small up to *ca.* 200 mTorr. Similar experiments were performed using $O_2$:$H_2O$ ratios which ranged from 0.8 to 17. In all cases, the experimentally determined OH• radical concentration was found to be in agreement with the expected equilibrium value.

Additional evidence for the reaction being in chemical equilibrium was obtained from the experimentally determined orders of reaction and the enthalpy of reaction. The observed reaction orders of 0.25 and 0.50 for $O_2$ and $H_2O$, respectively, agree with the expected orders obtained from the law of mass action for the net reaction:

$$^1/_4\mathrm{O_2} + {}^1/_2\mathrm{H_2O} \rightleftharpoons \mathrm{OH^\bullet} \quad (5)$$

The enthalpy of this reaction, calculated using the thermodynamic data from the JANAF tables,[30] was $\Delta H = 38.98$ kcal/

**Table 1.** Quenching Rate Constants for Collisions between Electronically Excited Hydroxyl Radicals and Water, Oxygen, and Helium at Elevated Temperatures

| $k_{\mathrm{q}}$ (cm$^3$ molecules$^{-1}$ s$^{-1}$) | temp (K) | ref |
|---|---|---|
| | $H_2O$ | |
| $7.39 \times 10^{-10}$ | 1500−1800 | 24 |
| $6.21 \times 10^{-10}$ | 1100−1500 | 25 |
| $3.9 \times 10^{-10}$ | 1220 | 26 |
| $4.7 \times 10^{-10}$ | 1140 | 26 |
| $4.4 \times 10^{-10}$ | 1430 | 26 |
| $4.7 \times 10^{-10}$ | 1000 | 26 |
| $6.67 \times 10^{-10}$ | 1200−1800 | 27 |
| | $O_2$ | |
| $1.77 \times 10^{-10}$ | 1500−1800 | 24 |
| $1.10 \times 10^{-10}$ | 1100−1500 | 25 |
| $1.1 \times 10^{-10}$ | 1160 | 26 |
| $2.2 \times 10^{-10}$ | 1460 | 26 |
| $1.7 \times 10^{-10}$ | 1090 | 26 |
| $1.18 \times 10^{-10}$ | 1200−1800 | 27 |
| | He | |
| $5.6 \times 10^{-14}$ | 298 | 28 |

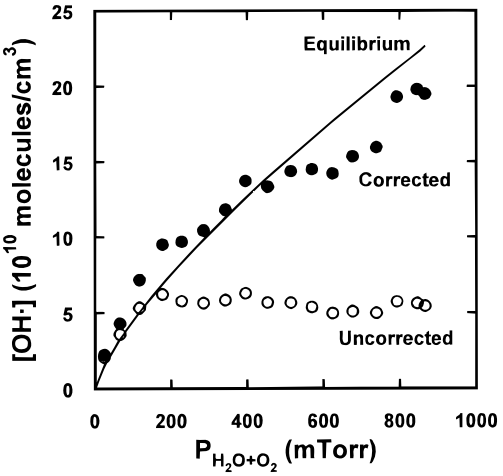


**Figure 3.** The concentration of OH• radicals produced as a function of the sum of water and oxygen partial pressures. The oxygen to water ratio was 3.7:1.0, the amount of $La_2O_3$ was 27 mg, and the temperature was 900 °C. Collisional quenching becomes significant above 200 mTorr as shown by the comparison between the uncorrected data (○) and the corrected data (●). The experimentally determined concentration, when corrected for collisional quenching, is the same as the calculated equilibrium concentration (—) within experimental error.

(20) McGee, T. J.; McIlrath, T. J. *J. Quant. Spectrosc. Radiat. Transfer* **1984**, *32*, 179−184.
(21) Goldman, A.; Gillis, J. R. *J. Quant. Spectrosc. Radiat. Transfer* **1981**, *25*, 111−135.
(22) Chidsey, I. L.; Crosley, D. R. *J. Quant. Spectrosc. Radiat. Transfer* **1980**, *23*, 187−199.
(23) Crosley, D. R.; Chidsey, I. L. Tables of Calculated Transition Probabilities for the A−X System of OH. *Ballistic Research Laboratory Report*, **1981,** ARBRL-TR-02326.
(24) Hooymayers, H. P.; Alkemade, C. T. J. *J. Quant. Spectrosc. Radiat. Transfer* **1967**, *7*, 495−504.
(25) Carrington, T. *J. Chem. Phys.* **1958**, *30*, 1087−1095.
(26) Fairchild, P. W.; Smith, G. P.; Crosley, D. R. *J. Chem. Phys.* **1983**, *79*, 1795−1807.
(27) Hidaka, Y.; Kawano, H.; Suga, M. *Bull. Chem. Soc. Jpn.* **1983**, *56*, 923−924.
(28) Hogan, P.; Davis, D. D. *J. Chem. Phys.* **1975**, *62*, 4574−4576; Lengel, R. K. C.; Crosley, D. R. *J. Chem. Phys.* **1976,** *64*, 3900−3901; Hogan, P.; Davis, D. D. *J. Chem. Phys.* **1976,** *64*, 3901.
(29) Penndorf, R. *J. Opt. Soc. Am.* **1957**, *47*, 176−182.
(30) *JANAF Thermochemical Tables*, 2nd ed.; National Standard Reference Data Service, 1971.

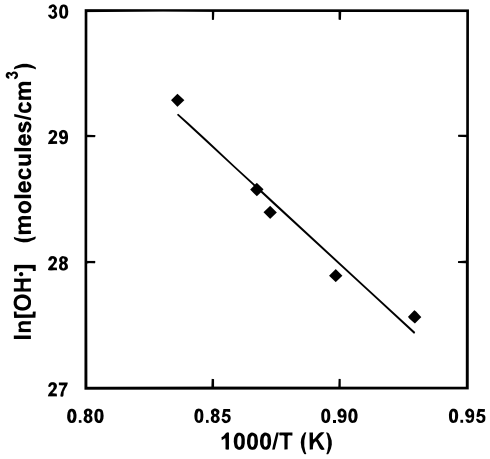


**Figure 4.** The logarithm of OH• radical concentration as a function of 1000/*T*. $\Delta H$ was 37.0 ± 3.8 kcal/mol with 750 mTorr of $O_2$ and 200 mTorr of $H_2O$ over 27 mg of $La_2O_3$.

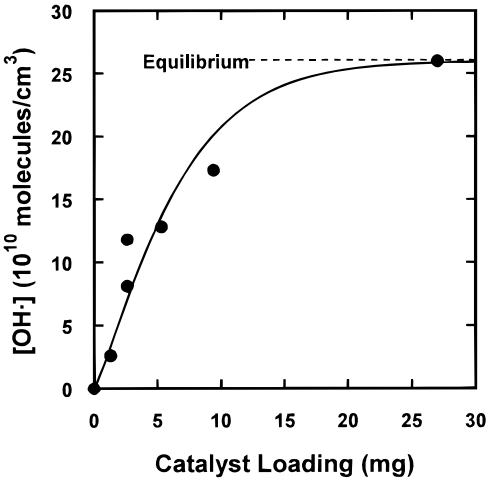


**Figure 5.** Effect of catalyst loading on the concentration of OH• radicals over $La_2O_3$ at 900 °C with 750 mTorr of $O_2$ and 200 mTorr of $H_2O$. At the highest loadings, the concentration was the same as the calculated equilibrium value within experimental error.

mol at 1200 K. The experimentally determined enthalpy of reaction, determined from the results of Figure 4, was 37.0 ± 3.8 kcal/mol, which is in good agreement with the calculated value. The logarithm of the OH• radical concentration was plotted instead of ln K since the equilibrium for reaction 5 lies far to the left. Thus, it is concluded that at large catalyst loadings and at reactant pressures up to 1 Torr, hydroxyl radicals are in chemical equilibrium with water and oxygen over $La_2O_3$. This result is the same as was previously found at pressures less than 100 mTorr.

**Kinetically Controlled Production of OH• Radicals.** Of more interest in the present study were the conditions under which the reaction is *not* in chemical equilibrium, because of the insight that could be gained concerning the reaction mechanism and activities of the respective catalysts. In order to operate in a kinetically controlled regime, the amount of catalyst placed onto the quartz frit was decreased. As shown in Figure 5, the concentration of hydroxyl radicals increased as the amount of $La_2O_3$ catalyst was increased from 0 to 27 mg. At the latter loading, the OH• radical concentration was equivalent to the equilibrium value. In addition to demonstrating the deviation from chemical equilibrium, Figure 5 also shows that the production of OH• radicals involves the entire catalyst. The linear relationship between loading and concentration observed for ≤5 mg of $La_2O_3$ clearly indicates that more than

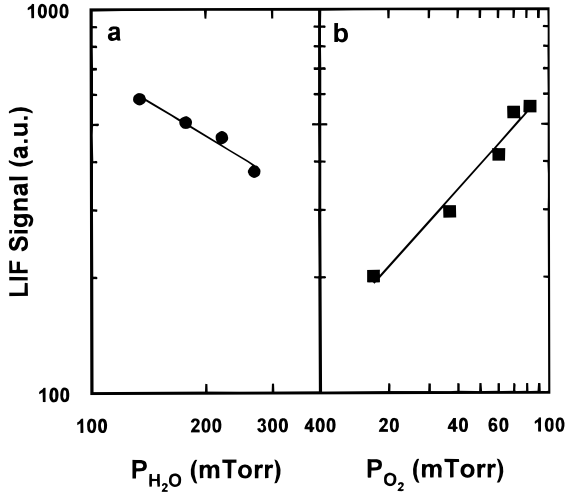


**Figure 6.** The effect of water and oxygen partial pressures on the concentration of OH• radicals: (a) using 657 mTorr of $O_2$ and 2.6 mg of $La_2O_3$ at 902 °C, the order of reaction with respect to water was −0.60 ± 0.09; (b) using 23.1 mTorr of $H_2O$ and 2.6 mg of $La_2O_3$ at 900 °C, the order of reaction with respect to oxygen was 0.67 ± 0.06.

just the outermost surface layer of the catalyst is involved in OH• radical production. It should also be noted that in the absence of a catalyst there was no measurable amount of OH• radicals. When the catalyst was placed on the upstream side of the quartz frit, no radicals were detected, which suggests that the OH• radicals rapidly react with an $SiO_2$ surface.

Further evidence for the reaction being in a kinetically controlled regime at low catalyst loading was provided by both the reaction orders and the activation energies. The orders of reaction at 900 °C and with 2.7 mg of $La_2O_3$ were obtained from the data shown in Figure 6. The order with respect to water, at 657 mTorr of $O_2$, was −0.60 ± 0.09; with 23.1 mTorr of $H_2O$, the order of reaction with respect to oxygen was 0.67 ± 0.06. These orders are very different from the respective stoichiometric coefficients of reaction 5. The reaction orders can be understood by considering the following modified form of the mechanism that has previously been used to explain the formation of OH• radicals on lanthanide oxides:

$$H_2O + O_S^- \rightleftharpoons OH^\bullet + OH_S^- \quad (6)$$

$$2OH_S^- \rightleftharpoons H_2O + \square + O_S^{2-} \quad (7)$$

$$O_2 \rightleftharpoons 2O_S \quad (8)$$

$$O_S + \square + O_S^{2-} \rightleftharpoons 2O_S^- \quad (9)$$

where "□" refers to an oxygen vacancy and the subscript "s" refers to a surface species. Reaction 7 is a well-known process by which surface hydroxides are lost as water. Although a simple bimolecular reaction between two surface hydroxide ions is indicated, the reaction probably involves a proton from one hydroxide ion reacting with a second hydroxide ion. Reaction 7 should be rapid at 900 °C.[31] Reaction 6 is analogous to one that has been proposed for the formation of $CH_3^\bullet$ radicals over lithium-modified MgO catalysts, for which there is ESR evidence for $O^-$ centers.[32] Islam et al.[33] have carried out

(31) Cant, N. W.; Lukey, C. A.; Nelson, P. F.; Tyler, R. J. *J. Chem. Soc., Chem. Commun.* **1988**, 766−768.
(32) Ito, T.; Wang, J.-X.; Lin, C.-H.; Lunsford, J. H. *J. Am. Chem. Soc.* **1985**, *107*, 5062−5068.
(33) Islam, M. S.; Ilett, D. J.; Parker, S. C. *J. Phys. Chem.* **1994**, *98*, 9637−9641.

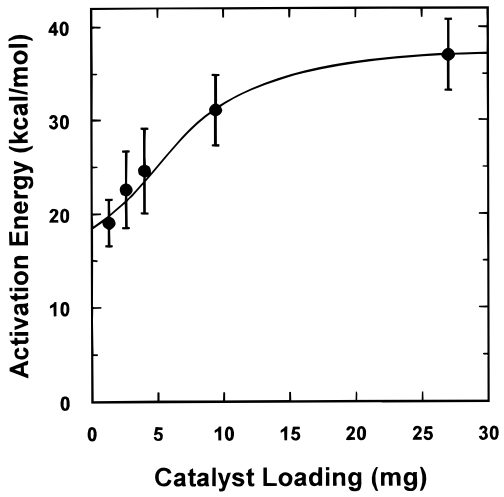


**Figure 7.** Effect of catalyst loading on the observed activation energy: 740 mTorr of $O_2$ and 210 mTorr of $H_2O$ were allowed to react over $La_2O_3$.

**Table 2.** Comparison of the Production of Hydroxyl Radicals over Various Catalysts with 740 mTorr of Oxygen, 210 mTorr of Water, and a Temperature of 900 °C[a]

| catalyst | loading (mg) | [OH•] ($10^{10}$ molecules/cm$^3$) | rate ($10^{12}$ molecules/g·s) |
|---|---|---|---|
| $La_2O_3$ | 2.7 | 9.9 | 18.7 |
| $Nd_2O_3$ | 2.7 | 6.2 | 9.6 |
| $Sm_2O_3$ | 2.8 | 4.0 | 6.5 |
| $Yb_2O_3$ | 16.9 | 0.93 | 0.23 |
| $CeO_2$ | 38.3 | none | none |
| MgO | 8.0 | 3.0 | 1.4 |

[a] At equilibrium the concentration of OH• is $2.6 \times 10^{11}$ molecules/cm$^3$.

theoretical studies on $La_2O_3$ and have concluded that the formation of $O^-$ pairs requires an energy of only 0.10 eV. The centers also require the presence of oxide ion vacancies and molecular oxygen. Consistent with this result, Mirodatos and co-workers[34] have shown that the activation of $CH_4$ over $La_2O_3$ involves a special form of oxygen that is in equilibrium with gas-phase molecular oxygen, such as described by reactions 8 and 9. A reaction order of 0.5 with respect to $O_2$ would be consistent with reaction 8 being at equilibrium, followed by a slow step that could be reaction 9. A reaction order of 0.67 suggests that reaction 8 may not quite be at equilibrium. The negative order in $H_2O$ indicates that water may be removing oxygen vacancies at the surface via the reverse of reaction 7 and thus impeding reaction 9, i.e., the rate of $O^-_s$ formation.

As shown in Figure 7, as the amount of catalyst was reduced, the observed activation energy decreased from 37 kcal/mol, until it reached a lower limit of approximately 18 kcal/mol. This latter energy is much lower than the enthalpy of the reaction, supporting the conclusion that the reaction is in a kinetically controlled regime. It is unusual that the activation energy did not reach some constant value at the smaller catalyst loadings, but, in fact, may have done so within experimental error.

Other catalysts were also studied under kinetically controlled conditions, and the results obtained with $La_2O_3$, $Nd_2O_3$, $Sm_2O_3$, $Yb_2O_3$, $CeO_2$, and MgO are compared in Table 2. Magnesium oxide was included in this group because it has been shown to be effective in the catalytic combustion of methane.[35] The data are reported as concentrations of OH• radicals, and it is evident that in all cases they are well below the equilibrium concentrations at the conditions indicated. The loadings were essentially the same for the first three, more active, oxides, but for the less active oxides the loadings were increased. The rate of OH• radical formation for the lanthanide oxides followed the order $La_2O_3 > Nd_2O_3 > Sm_2O_3 > Yb_2O_3 \gg CeO_2$, which corresponds to the order of basicity for these materials. Moreover, it is the same order as that found for the formation of $CH_3$• radicals,[17] which is not surprising since the same type of active center is believed to be responsible for radical formation in both cases. It is evident that MgO falls between $Yb_2O_3$ and $Sm_2O_3$ in its ability to generate OH• radicals. Since the radicals collide with the metal oxide surfaces many times before they exit the catalyst and are detected in the gas phase, the net rates that are reported reflect both the formation rate and the removal rate due to secondary reactions.

**Potential Role of Surface-Generated OH• Radicals in Catalytic Combustion.** As discussed by Schmidt and co-workers,[2,3] surface generation or consumption of hydroxyl radicals can strongly affect homogeneous ignition and extinction of methane/air flames. Surface formation of hydroxyl radicals tends to promote homogeneous ignition. In this study, we were interested in determining whether the concentrations of hydroxyl radicals produced over a metal oxide surface (*e.g.* $La_2O_3$) might be significant in a combustion reaction. As a first-order approximation, it was assumed that one could obtain an equilibrium concentration of OH• radicals over a catalyst at significantly higher pressures. This concentration was then compared with that obtained in a model combustion reaction.

A batch model, which consists of 156 gas-phase reactions, has been successfully used to interpret the kinetic isotope effects that were observed during the oxidative coupling of methane.[36] In addition, it accurately reflects the experimental results that were obtained during the gas-phase oxidative dehydrogenation of ethane.[37] In this study, calculations were performed using this model to examine the role of hydroxyl radicals during methane combustion. The rate constants used in the model were taken from the National Institute of Science and Technology (NIST) data base.[38] The ACUCHEM computer program[39] was used to determine the concentrations of all reactant species as a function of time. At the beginning of the calculation, the $CH_4$ and $O_2$ pressures were taken to be 72.2 and 144.4 Torr, respectively, and the temperature was 900 °C. The OH• radical concentration increased to a maximum value of $3.3 \times 10^{12}$ molecules/cm$^3$, at which point the corresponding $O_2$ and $H_2O$ pressures were 122 and 28 Torr, respectively. At these same pressures of $O_2$ and $H_2O$, the *equilibrium* OH• radical concentration is $1.1 \times 10^{13}$ molecules/cm$^3$. The fact that the equilibrium concentration is considerably greater than the maximum concentration obtained during the reaction suggests that these surface-generated radicals may indeed be important in the catalytic combustion of $CH_4$ via heterogeneous−homogeneous reactions.

With respect to oxidative coupling of methane, which usually is carried out in the 700−800 °C temperature range, a model similar to the one described by Shi *et al.*[36,40] indicated that surface-generated hydroxyl radicals would increase the conver-

(34) Lacombe, S.; Zanthoff, H.; Mirodatos, C. *J. Catal.* **1995**, *155*, 106−116.
(35) Berg, M.; Järås, S. *Appl. Catal. A: General* **1994**, *114*, 227−241.
(36) Shi, C.; Xu, M.; Rosynek, M. P.; Lunsford, J. H. *J. Phys. Chem.* **1993**, *97*, 216−222.
(37) Lunsford, J. H.; Morales, E.; Dissanayake, D.; Shi, C. *Int. J. Chem. Kinet.* **1994**, *26*, 921−928.
(38) Westley, F.; Herron, J. T.; Cvetanoic, R. J.; Hampson, R. F.; Mallard, G. *NIST Chemical Kinetics Database,version 3.0,* **1991,** National Institute of Standards and Technology, U. S. Dept. of Commerce.
(39) Braun, W.; Herron, J. T.; Kahaner, D. K. *Int. J. Chem. Kinet.* **1988**, *20*, 51−62.
(40) Shi, C.; Hatano, M.; Lunsford, J. H. *Catal. Today* **1992**, *13*, 191−199.

sion of methane, but at comparable levels of conversion the $CO_x$ selectivity would not be significantly altered. Thus, the positive effect of $OH^{\bullet}$ radicals in abstracting a hydrogen atom from $CH_4$, and thereby generating more $CH_3^{\bullet}$ radicals, appears to be balanced by the formation of more $CO_x$ via secondary reactions.

## Conclusions

The more basic lanthanide oxides and magnesium oxide are very active at 900 °C for the formation of $OH^{\bullet}$ radicals from the reaction of $O_2$ and $H_2O$. The hydroxyl radicals are formed on the surface and emanate into the gas phase at rates that may be significant in catalytic combustion reactions. The abstraction of hydrogen from $H_2O$ is analogous to the abstraction of hydrogen from $CH_4$ during the formation of $CH_3^{\bullet}$ radicals over these same catalysts. Under kinetically controlled conditions, it appears that oxygen incorporation at surface sites may be the rate limiting step in the catalytic cycle.

**Acknowledgment.** This research was supported by the Office of Basic Energy Sciences, U.S. Department of Energy.

JA960566G